

OR2-3

液柱マランゴニ対流内の粒子集合構造のトモグラフィック再構築

Tomographic Reconstruction of Particle Accumulation Structure in a Thermocapillary Liquid Bridge

矢野大志¹, 中西裕二¹, 西野耕一²

Taishi YANO¹, Yuji NAKANISHI¹ and Koichi NISHINO²

¹神奈川大学, Kanagawa University

²横浜国立大学, Yokohama National University

1. Introduction

Since the thermocapillarity—the force due to surface tension difference caused by the temperature gradient along the liquid-gas interface—can be the primally source for the liquid motion under the reduced-gravity environment, numerous hydrodynamic experiments related to this phenomenon have been conducted under microgravity (μg , hereinafter) in the past few decades. The thermocapillarity-driven convection (referred to hereinafter as the thermocapillary convection) in a high-Prandtl-number liquid bridge is one of the most famous research themes in the Japanese Experiment Module Kibo onboard the International Space Station (ISS), and several series of μg experiments—i.e., the so-called MEIS, Marangoni UVP, and Dynamic Surf projects—had been performed in the period from 2008 to 2020 in the Kibo module^{1,2}). As shown in **Figure 1**, there exists a pair of disks of diameter D with the gap H open, and a column of liquid (i.e., silicone oil in this case) is suspended between these disks. The upper disk is set warmer than the lower disk, and the temperature difference $\Delta T (= T_H - T_C)$ given to these disks drives the toroidal thermocapillary convection as illustrated in **Figure 1**, where T_C and T_H are the temperatures of cooler disk and warmer disk, respectively. Hereinafter, the disk with lower/higher temperature is referred to as the cold/hot disk. One of the most interesting features of thermocapillary convection in a high-Prandtl number liquid bridge is the transition of the flow from a steady

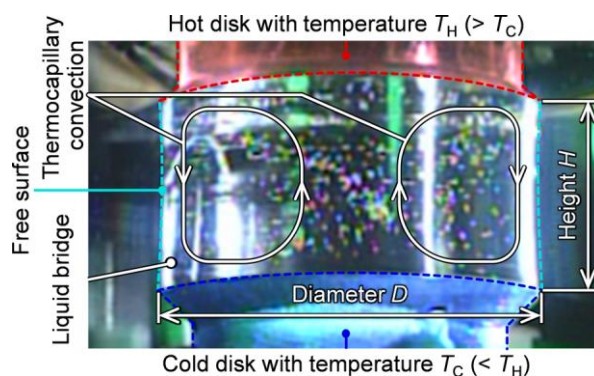


Figure 1. Liquid bridge formed in the μg experiment.

state to an oscillatory state at a certain instability threshold^{3,4}). The thermocapillary convection after the transition to the oscillatory state shows a variety of spatially complex structures. Furthermore, under some special conditions, oscillatory thermocapillary convections involve the structure of tracer particles accumulating along a single or multiple narrow paths, which is called the particle accumulation structure (PAS, hereinafter)⁵⁻⁸). In this study, the PAS observed in the previous μg experiment is visualized by means of the tomographic reconstruction⁹) to understand its formation process.

2. Tomographic Reconstruction

In the experimental cells used in the μg projects mentioned above, there existed three CCD cameras on top of the liquid bridge²). Since the hot disk, along with the sensors and heaters embedded in it, were all transparent, the CCD cameras could observe the flow inside the liquid bridge without being affected by refraction and reflection at the free surface. There were a few dozen reference points marked on the liquid-contact surface of the cold disk. These reference points were used to obtain camera parameters that relate two-dimensional (2-D, hereinafter) coordinate systems on images and a three-dimensional (3-D, hereinafter) coordinate system in space pinned to the liquid bridge¹⁰). In the μg experiments conducted aboard the Kibo module, many fine tracer particles were seeded in a liquid bridge for flow visualization. Their 2-D positional information taken by each CCD camera can be reconstructed into 3-D distributional ones by means of image tomography⁹) using camera parameters.

In the μg experiments conducted aboard the Kibo, a rich variety of oscillatory thermocapillary convection was observed under various experimental conditions; however, that involving the PAS was very limited. The target μg experiment in this study is the third series of Dynamic Surf project conducted in 2015–2016 (i.e., Dynamic Surf-3), in which PASs were observed in a few experimental runs. The test liquid was a 10-cSt silicone oil with the kinematic viscosity of $\nu = 10.0 \times 10^{-6} \text{ m}^2/\text{s}$, the thermal diffusivity of $\kappa = 8.94 \times 10^{-8} \text{ m}^2/\text{s}$, and the resultant Prandtl number of $\text{Pr} (= \nu/\kappa) = 112$ at $25 \text{ }^\circ\text{C}$ ²). The PAS having an azimuthal mode number of $m = 1$ was observed in the liquid bridge of $D = 30 \text{ mm}$, $A_r = 0.50$, and $V_r = 0.95$, when the temperature conditions were set at $T_c = 40.0 \text{ }^\circ\text{C}$ and $T_H = 48.2 \text{ }^\circ\text{C}$, where $A_r (= H/D)$ and $V_r (= V/(\pi D^2 H/4))$ are the aspect ratio and the volume ratio (i.e., the ratio of the liquid volume V to the cylindrical gap volume $\pi D^2 H/4$), respectively. The present study is targeted at reconstructing this PAS. To reach this goal, the 3-D space in which the liquid bridge exists is discretized into many volume elements (i.e., voxels) as shown in **Figure 2**(a). We note that the

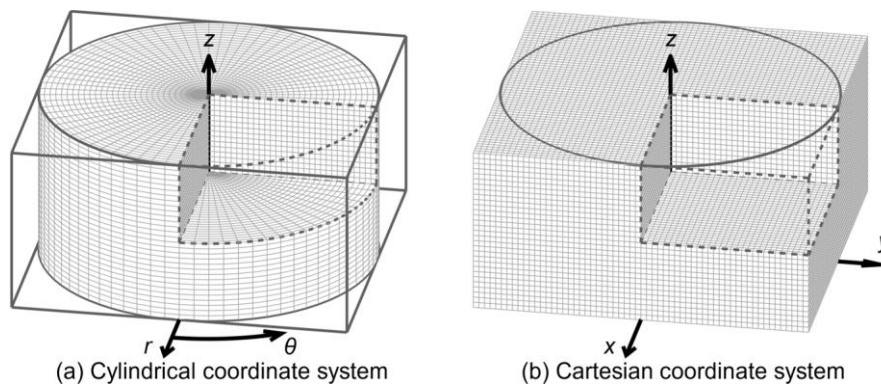


Figure 2. Voxel configurations for the liquid bridge with $A_r = 0.50$ discretized in (a) the cylindrical coordinate system and (b) the cartesian coordinate system.

target domain is, in fact, discretized more finely, but the voxel configuration is illustrated roughly in this figure for better visibility. The cylindrical domain is divided equally into (150, 360, 150) in the (r, θ, z) directions in a cylindrical coordinate system, resulting in triangular prismatic and trapezoidal prismatic voxels in shape and 8.1 million voxels in the total number. Actually, the triangular prismatic voxels exist only in the part adjacent to the z -axis, and the most part is occupied with the trapezoidal prismatic voxels. In the general tomographic reconstruction^{9,11}, the measurement domain is divided into rectangular prismatic voxels in a Cartesian coordinate system as shown in **Figure 2(b)**. As mentioned above, the present tomographic reconstruction is performed with nonrectangular prismatic voxels, which is, to the best of authors' knowledge, the first attempt except for the earlier work of this study¹². The use of a cylindrical coordinate system as well as voxels with axisymmetric shape can reduce computational costs (or improve spatial resolution) by eliminating unnecessary regions (i.e., the outer region of the cylinder in **Figure 2(b)**) because the target domain has cylindrical shape. Additionally, since the thermocapillary convection involving the PAS has an axisymmetric structure, it is favorable in postprocessing such as averaging in a rotating frame of reference.

The principal of tomographic reconstruction is basically independent on the shape of voxel; therefore, only its brief introduction is provided here. Firstly, define the initial intensity of each voxel (i.e., E at $n = 0$), and update it by using the following multiplicative algebraic reconstruction technique (MART, hereinafter)⁹:

$$E_i(n) = E_i(n-1) \prod_k \prod_j \left[\frac{I_j^{(k)}}{\sum_{i=1}^{N_{vx}} \{w_{ij}^{(k)} E_i(n-1)\}} \right]^{\mu w_{ij}^{(k)}}, \quad (1)$$

where i, j , and k are, respectively, the voxel number, the pixel number, and the camera number; N_{vx} , N_{px} , and N_{cam} are, respectively, the numbers of voxel, pixel, and camera; I is the image intensity; w_{ij} is the weighting coefficient representing the contribution of the i -th voxel to the j -th pixel; and μ is the relaxation parameter. As described above, $N_{vx} = 8.1 \times 10^6$ and $N_{cam} = 3$. The size of image used in this study is 720×480 pixels, giving $N_{px} \approx 3.5 \times 10^5$. The value of w_{ij} is evaluated by the Monte Carlo method¹³, but its details are not covered here. We note that the contributions of camera parameters are contained in w_{ij} . The initial condition is arbitrary (e.g., a uniform non-zero value). In this study, it is determined as

$$E_i(0) = \prod_k \prod_j \left\{ w_{ji}^{(k)} I_j^{(k)} \right\}, \quad (2)$$

where w_{ji} is the weighting coefficient representing the contribution of the j -th pixel to the i -th voxel and is also evaluated by the Monte Carlo method. Using equations (1) and (2), one can reconstruct the 3-D distribution of tracer particles in a liquid bridge from 2-D particle images.

3. Results and Discussion

Figure 3 shows an example of the PAS observed in Dynamic Surf-3, which are obtained by phase averaging over 1000 original particle images after background subtraction. Since the flow field is rotating at a constant period (i.e., 32.8 s) in this case, the phase averaging can remove (or dilute) non-accumulated tracer particles while leaving accumulated ones. We note that the actual tracer particles appear white in a dark background;

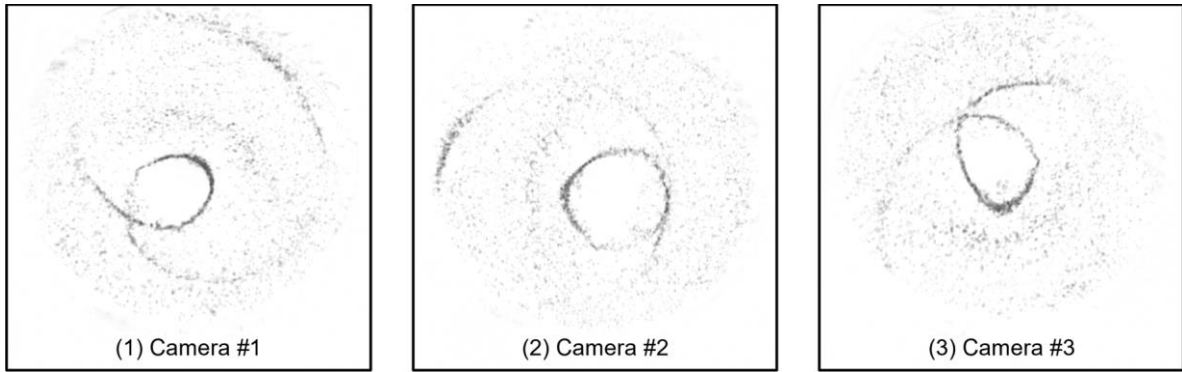


Figure 3. Particle images used for the tomographic reconstruction. The black and white is reversed in each image to improve visibility.

however, the monochrome is inverted in **Figure 3** to improve the visibility. The 3-D distribution of tracer particles reconstructed from the particles images in **Figure 3** is shown in **Figure 4(a)**. Although, the tracer particles are elongated in the negative z -direction and the result seems noisy, it can be said that the tomographic reconstruction has been done adequately. Especially, the positional accuracy in the in-plane direction (i.e., r and θ) is good. In order to make the structure of PAS much clearer, the tomographic reconstruction is carried out for continuous data, and the time series of 3-D distributions of tracer particles are averaged in a rotating frame of reference. The result is shown in **Figure 4(b)**. This rotational averaging enhances the contrast between accumulated and non-accumulated tracer particles, and one can recognize that the path of accumulating particles rises from the cold disk towards the hot disk while swirling in a clockwise direction. This PAS seems to be opened in the present result because it is difficult to capture tracer particles near the free surface; however, it is expected to be closed according to the previous studies⁶⁻⁸). In any case, it can be said that the present tomographic reconstruction is effective for understanding the PASs.

4. Summary

The tomographic reconstruction technique dedicated to the thermocapillary convection in a cylindrical liquid bridge is developed, and the particle accumulation structure (PAS) is visualized. The measurement volume is divided into millions of trapezoidal prismatic and triangular prismatic voxels in a cylindrical coordinate system in the present tomographic reconstruction. The multiplicative algebraic reconstruction technique (MART), which is customized for the present study, is used to obtain the distribution of tracer particles in a thermocapillary liquid bridge. In Dynamic Surf-3—one of the series of μg experiments conducted

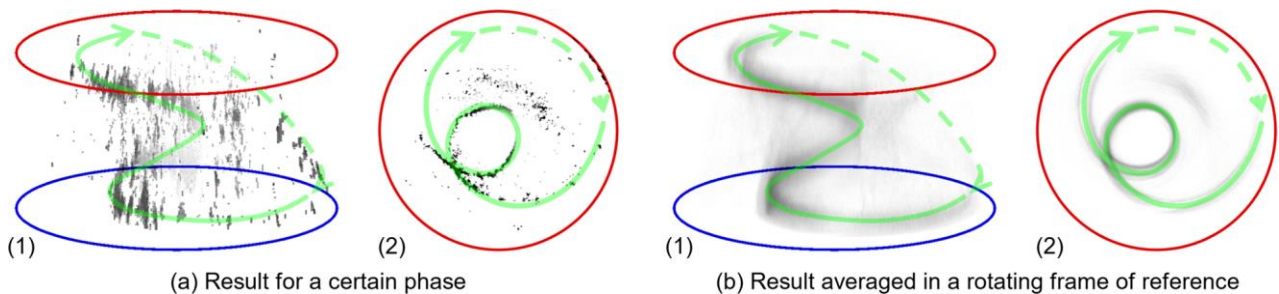


Figure 4. Distribution of tracer particles reconstructed by means of image tomography: (a) result for a certain phase and (b) result averaged in a rotating frame of reference. Each of (1) and (2) show bird's-eye view and r - θ cross-sectional view, respectively. The green curves are eye guides for the particle-accumulated path.

aboard the Kibo module onboard the International Space Station, the PAS was observed in a thermocapillary liquid bridge of $A_r = 0.50$ and $V_r = 0.95$ under the temperature conditions of $T_c = 40.0$ °C and $T_H = 48.2$ °C, and this PAS is reconstructed by the optical tomography developed in this study. The spiral path of accumulating tracer particles rising from the cold disk toward the hot disk is well recognized, especially the result averaged in a rotating frame of reference exhibits good observation. The developed tomographic reconstruction technique and the present results will hopefully help researchers to understand the details of PAS in a thermocapillary liquid bridge.

References

- 1) K. Nishino, T. Yano, H. Kawamura, S. Matsumoto, I. Ueno and M.K. Ermakov: Instability of thermocapillary convection in long liquid bridges of high Prandtl number fluids in microgravity. *J. Cryst. Growth*, **420** (2015) 57, DOI: [10.1016/j.jcrysgro.2015.01.039](https://doi.org/10.1016/j.jcrysgro.2015.01.039).
- 2) T. Yano, K. Nishino, S. Matsumoto, I. Ueno, A. Komiya, Y. Kamotani and N. Imaishi: Report on microgravity experiments of dynamic surface deformation effects on Marangoni instability in high-Prandtl-number liquid bridges. *Microgravity Sci. Technol.*, **30** (2018) 599, DOI: [10.1007/s12217-018-9614-9](https://doi.org/10.1007/s12217-018-9614-9).
- 3) H.C. Kuhlmann and H.J. Rath: Hydrodynamic instabilities in cylindrical thermocapillary liquid bridges. *J. Fluid Mech.*, **247** (1993) 247, DOI: [10.1017/S0022112093000461](https://doi.org/10.1017/S0022112093000461).
- 4) M. Wanschura, V.M. Shevtsova, H.C. Kuhlmann and H.J. Rath: Convective instability mechanisms in thermocapillary liquid bridges. *Phys. Fluids*, **7** (1995) 912, DOI: [10.1063/1.868567](https://doi.org/10.1063/1.868567).
- 5) D. Schwabe, S. Tanaka, A. Mizev and H. Kawamura: Particle accumulation structure in time-dependent thermocapillary flow in a liquid bridge under microgravity. *Microgravity Sci. Technol.*, **18** (2006) 117, DOI: [10.1007/BF02870393](https://doi.org/10.1007/BF02870393).
- 6) H.C. Kuhlmann and F.H. Muldoon: Particle-accumulation structures in periodic free-surface flows: Inertia versus surface collisions. *Phys. Rev. E*, **85** (2012) 046310, DOI: [10.1103/PhysRevE.85.046310](https://doi.org/10.1103/PhysRevE.85.046310).
- 7) H.C. Kuhlmann and F.H. Muldoon: Understanding particle accumulation structures (PAS) in thermocapillary liquid bridges. *J. Jpn. Soc. Microgravity Appl.*, **29** (2012) 64, DOI: [10.15011/jasma.29.2.64](https://doi.org/10.15011/jasma.29.2.64).
- 8) T. Sakata, S. Terasaki, H. Saito, S. Fujimoto, I. Ueno, T. Yano, K. Nishino, Y. Kamotani and S. Matsumoto: Coherent structures of $m = 1$ by low-Stokes-number particles suspended in a half-zone liquid bridge of high aspect ratio: Microgravity and terrestrial experiments. *Phys. Rev. Fluids*, **7** (2022) 014005, DOI: [10.1103/PhysRevFluids.7.014005](https://doi.org/10.1103/PhysRevFluids.7.014005).
- 9) G.E. Elsinga, F. Scarano, B. Wieneke and B.W. van Oudheusden: Tomographic particle image velocimetry. *Exp. Fluids*, **41** (2006) 933, DOI: [10.1007/s00348-006-0212-z](https://doi.org/10.1007/s00348-006-0212-z).
- 10) T. Yano and K. Nishino: Flow visualization of axisymmetric steady Marangoni convection in high-Prandtl-number liquid bridges in microgravity. *Int. J. Microgravity Appl.*, **36** (2019) 360202, DOI: [10.15011/jasma.36.360202](https://doi.org/10.15011/jasma.36.360202).
- 11) F. Scarano: Tomographic PIV: principles and practice. *Meas. Sci. Technol.*, **24** (2013) 012001, DOI: [10.1088/0957-0233/24/1/012001](https://doi.org/10.1088/0957-0233/24/1/012001).
- 12) T. Yano, Y. Nakanishi and K. Nishino: Proceedings of the 34th International Symposium on Space Technology and Science (2023) 2023-h-09.



© 2023 by the authors. Submitted for possible open access publication under the terms and conditions of the Creative Commons Attribution (CC BY) license (<http://creativecommons.org/licenses/by/4.0/>).